Supplementary Information

Initiation reactivity of cyclic nitramines mixed crystals from the perspective of XPS application

Veerabhadragouda B. Patil[a*], Jhonatan Rodrigues Pereira[b], Jan Macák[b], Svatopluk Zeman[a*]

[a]Institute of Energetic Materials, Faculty of Chemical Technology, University of Pardubice, CZ-532 10 Pardubice, Czech Republic

[b]Center of Materials and Nanotechnologies (CEMNAT), Faculty of Chemical Technology, University of Pardubice, CZ-532 10 Pardubice, Czech Republic

S1 Materials

The chemicals used in the current work, n-butanol, chloroform, and dimethyl sulfoxide (DMSO), ethyl acetate, ethyl formate, acetone and n-heptane, are purchased from Lachner. Inc., Neratovice (Czechia) in a pure grade for mixed crystals preparation without further purification. The cis-1,3,4,6-tetranitrooctahydroimidazo-[4,5-d]imidazole or bicyclo-HMX (BCHMX) was prepared at the Institute of Energetic Materials as reported [1, 2]. It was recrystallized using solvent/antisolvent technique by acetone/water, and ε-2,4,6,8,10,12-hexanitro-2,4,6,8,10,12-hewxaazaisowurtzitane (ε-CL20) was a product of the Explosia Co. Pardubice pilot plant, crystallized using ethyl acetate/n-heptane solvents system; by this way the product was obtained with impact sensitivity of 6.4 J (before precipitation its solution in ethyl acetate treated with a little amount of P_2O_5 [3]).

S2 Preparation of Coagglomerated Crystals(CACs)

Basically, two methods have been used to prepare these crystals [4]:

(a) classical cocrystallization in a solvent/antisolvent system, namely ethyl acetate/n-heptane (sample CCs1) and ethylformate/n-heptane (sample CCs2).

(b) coagglomeration of the nitramines co-precipitates (from the DMSO/water system) in n-butanol or chloroform - a procedure [4, 5] Similar to the Slurry Method [6].

S2.1 Coagglomeration mechanism prediction of CL20/BCHMX CACs:

The obtained observations from PXRD, FTIR, Raman spectrums and DTA thermograms found that there will be a conversion of ϵ-CL20 to β-CL20 after undergoing interaction with BCHMX during the coagglomeration process. Also shown the predominant N-N stretching vibrations in CL20, equivalently opposite N-N bonding undergone maximum stretching with bending to locate both -NO_2 groups in opposite side sides with Z-order [7, 8]. These changes are indicated by taking

the 3D structures of both forms of the CL20 molecule in Scheme S1[9 - 11]. These changes might indicate that CL20 had undergone self-polymorphic modification of the molecule to adjust with BCHMX to form a stable crystal lattice. These stretched N-N bonds showed active intermolecular hydrogen bonds and Van der Waals interactions in CL20 cocrystal earlier reported [5, 7, 9, 10]. Based on all these precious observations and other results of earlier reported works, a possible mechanism of co-agglomeration may feasibly be predicted in the sense of proposed the CACs/CCs molecular structure of CL20/BCHMX shown in Scheme S1.

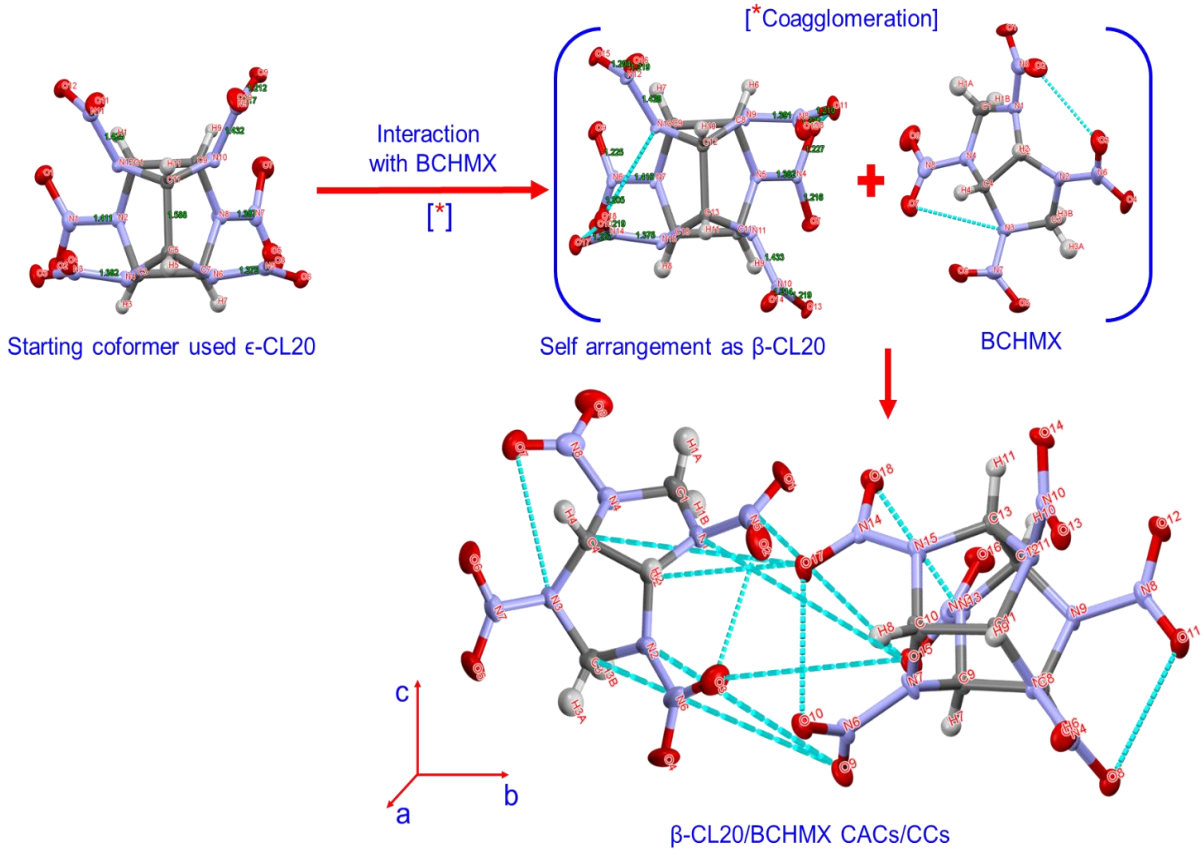

Scheme S1 Possible mechanism of coagglomeration interaction of both coformers in CACs/CCs [4]

S3 Experimental Part

S3.1 Hirshfeld surface analysis

The Crystal Explorer 3.0 (version 17.5) software tool was utilized to conduct an examination of the Hirshfeld surfaces(Figure 1) and the corresponding 2D fingerprint plots [11].

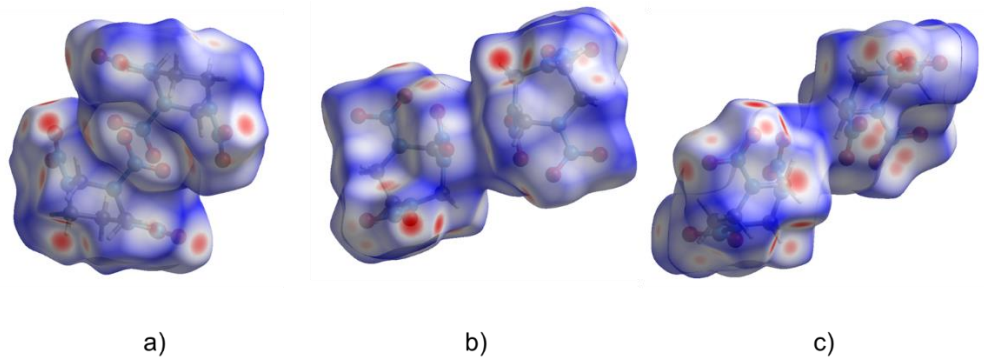

Fig. S2 Hirshfeld analysis for dimer of TTAZ molecule [12]

S3.2 X-ray Photoelectron Spectroscopy (XPS)

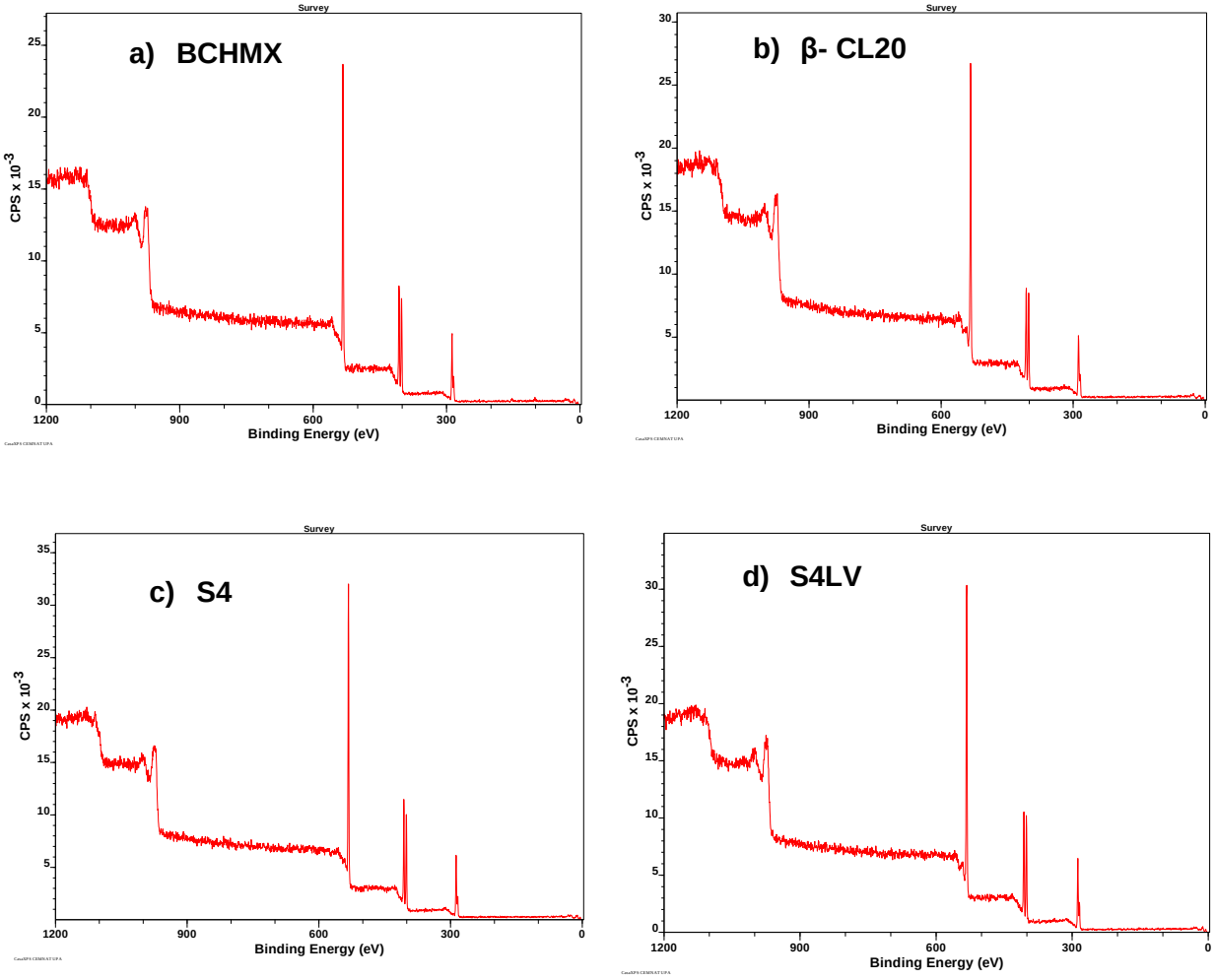

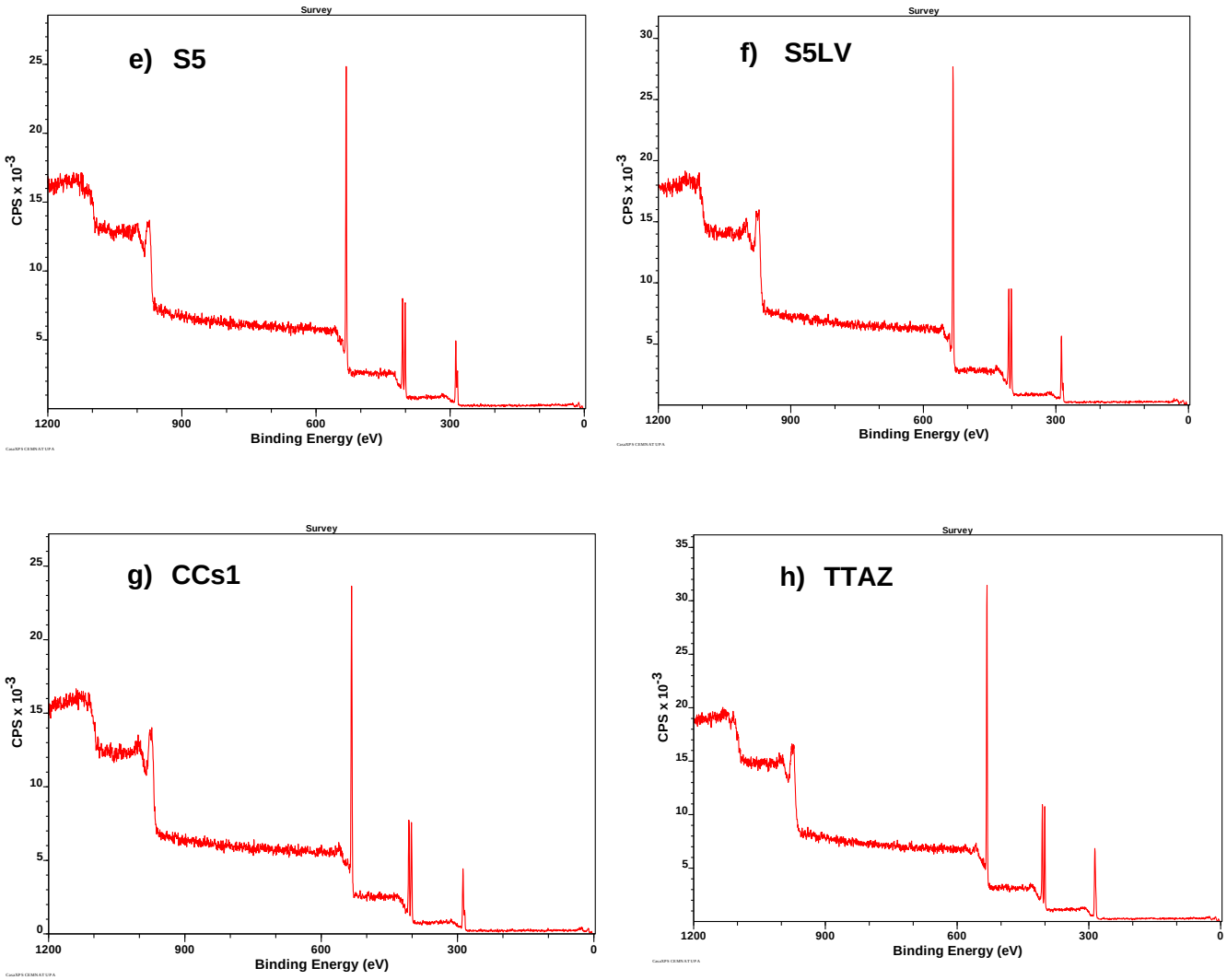

Fig. S3 (a - h) XPS Survey spectra of pure EMs and their CACs

a) BCHMX

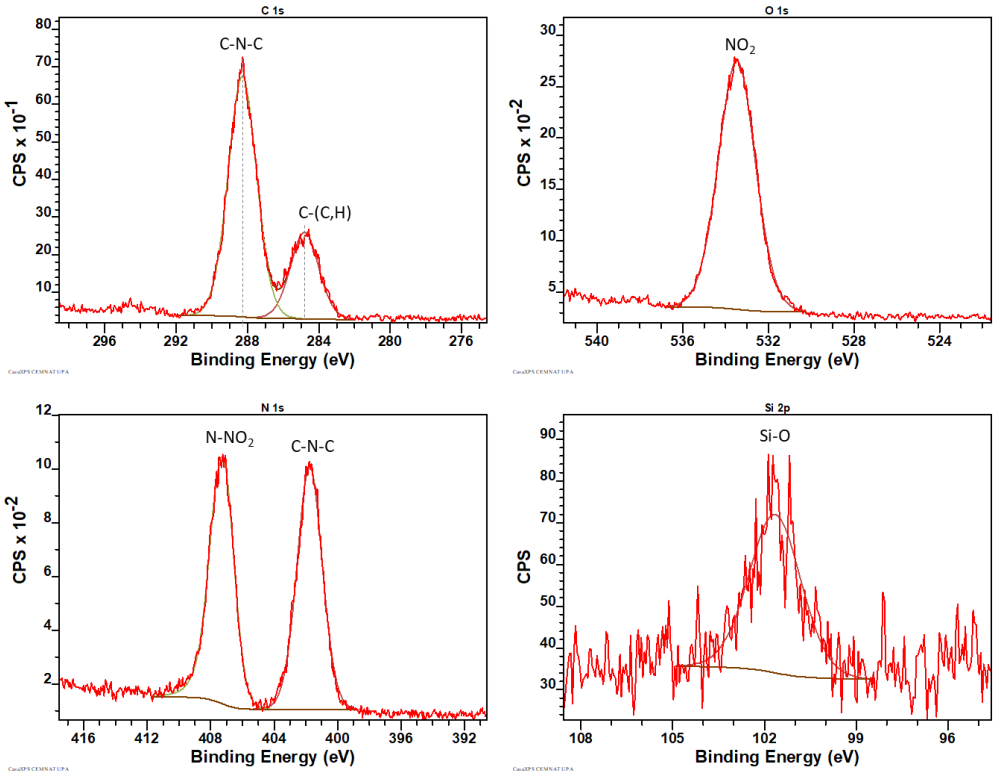

b) β- CL20

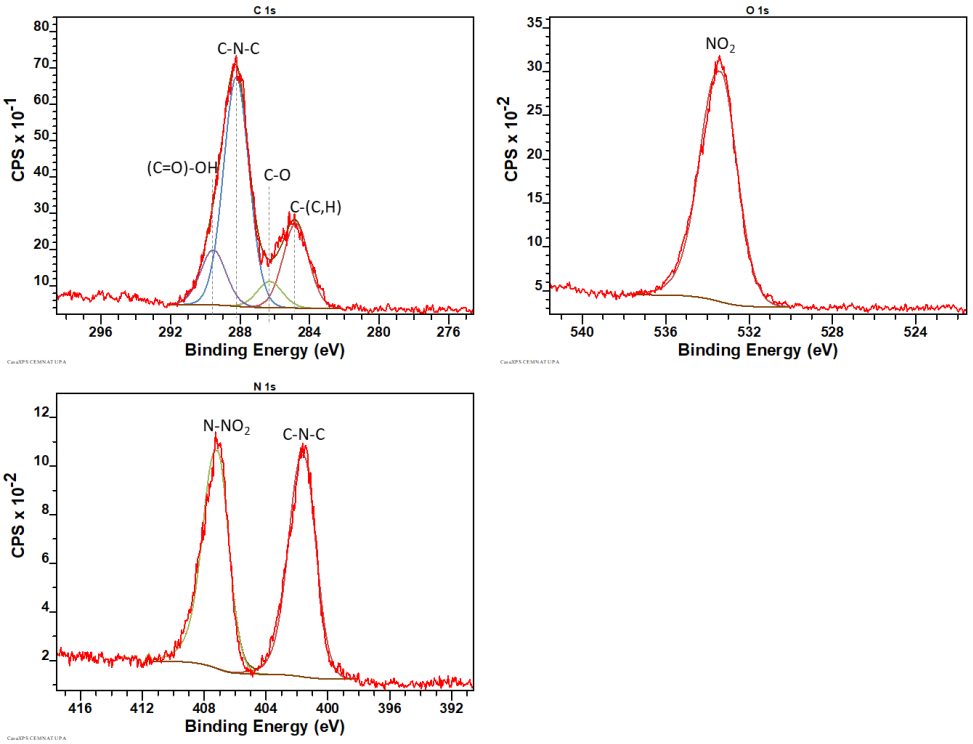

c) ε- CL20

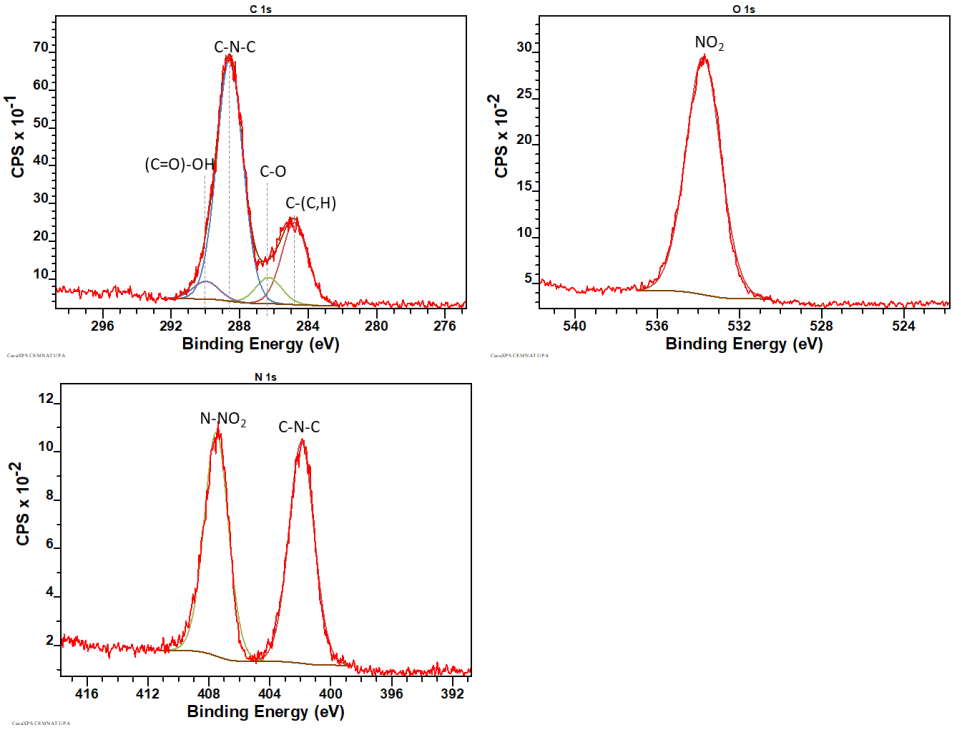
C 1s
C-N-C
(C=O)-OH
C-O
C-(C,H)
CPS x 10-1
Binding Energy (eV)
O 1s
NO2
CPS x 10-2
Binding Energy (eV)
N 1s
N-NO2
C-N-C
CPS x 10-2
Binding Energy (eV)

d) S4

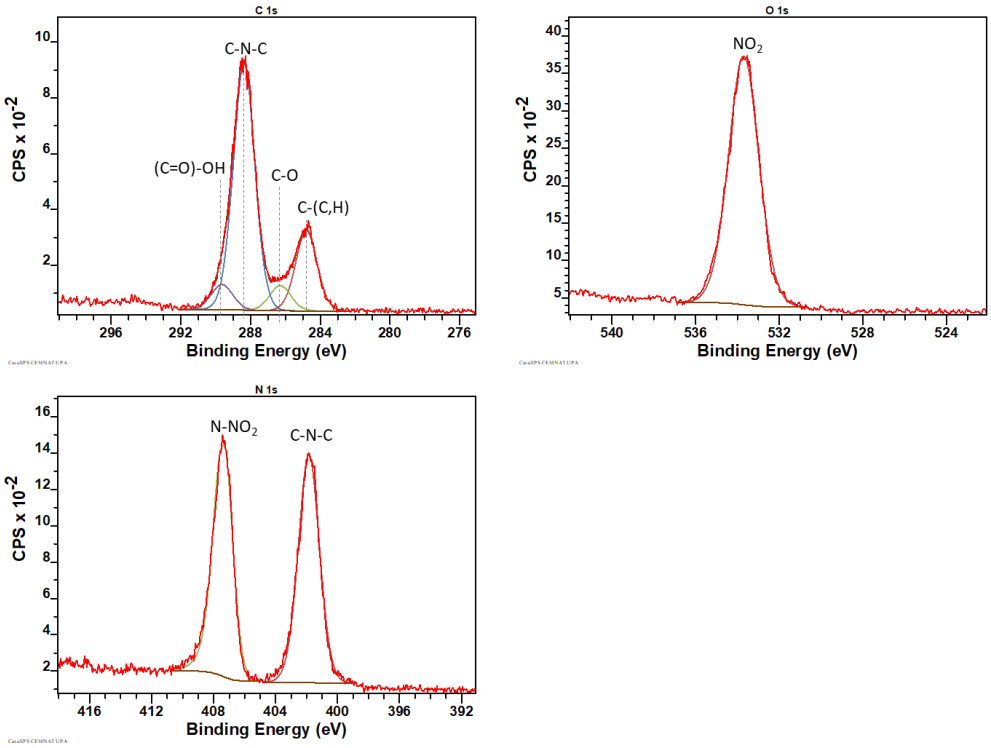
C 1s
C-N-C
(C=O)-OH
C-O
C-(C,H)
CPS x 10-2
Binding Energy (eV)
O 1s
NO2
CPS x 10-2
Binding Energy (eV)
N 1s
N-NO2
C-N-C
CPS x 10-2
Binding Energy (eV)

e) S4LV

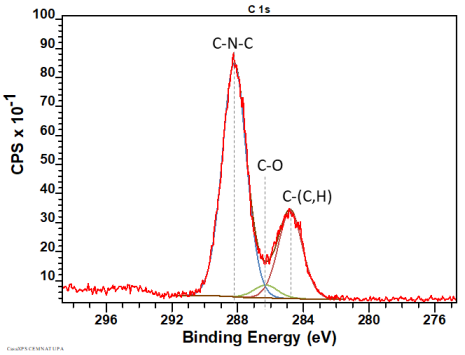
C 1s
C-N-C
C-O
C-(C,H)
CPS x 10-1
Binding Energy (eV)

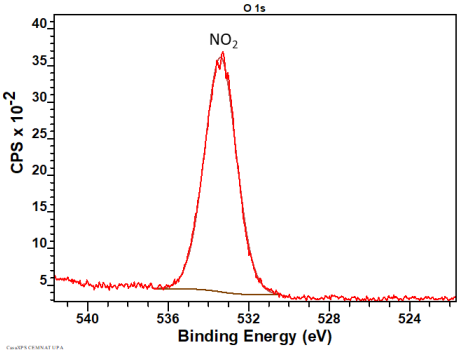
O 1s
NO2
CPS x 10-2
Binding Energy (eV)

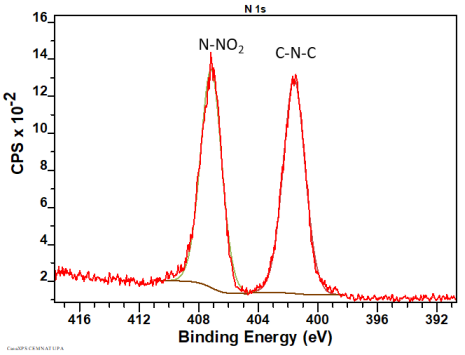
N 1s
N-NO2
C-N-C
CPS x 10-2
Binding Energy (eV)

f) S4LV

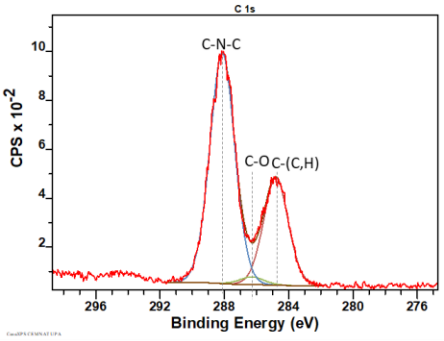
C 1s
C-N-C
C-O
C-(C,H)
CPS x 10-2
Binding Energy (eV)

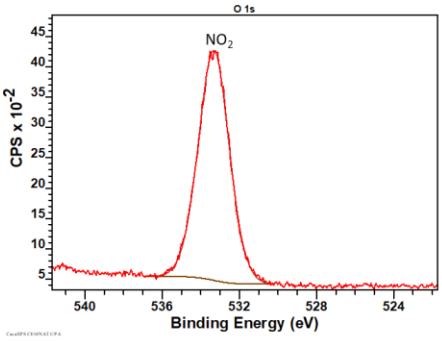
O 1s
NO2
CPS x 10-2
Binding Energy (eV)

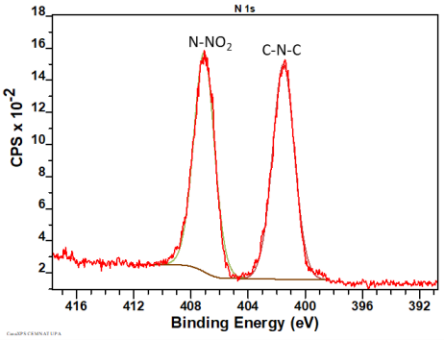
N 1s
N-NO2
C-N-C
CPS x 10-2
Binding Energy (eV)

g) S5

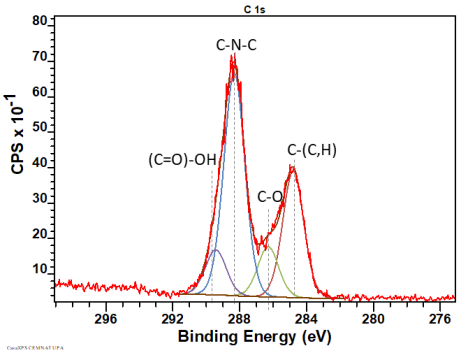
C 1s
C-N-C
(C=O)-OH
C-(C,H)
C-O
CPS x 10-1
Binding Energy (eV)

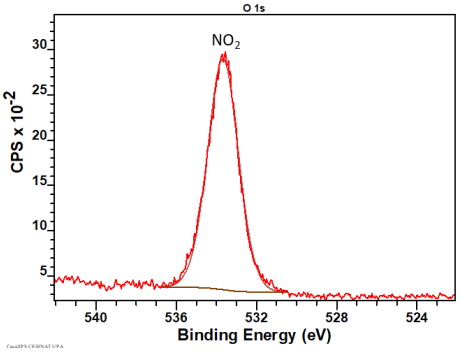
O 1s
NO2
CPS x 10-2
Binding Energy (eV)

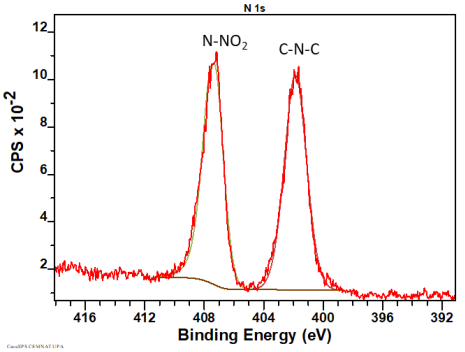
N 1s
N-NO2
C-N-C
CPS x 10-2
Binding Energy (eV)

h) S5LV

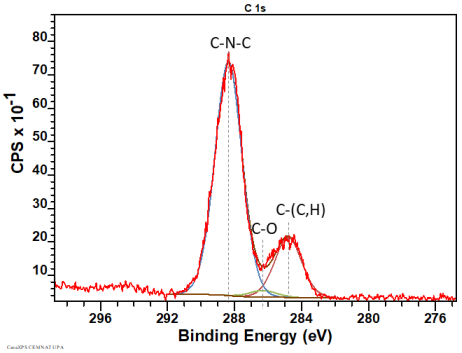
C 1s
C-N-C
C-(C,H)
C-O
CPS x 10-1
Binding Energy (eV)

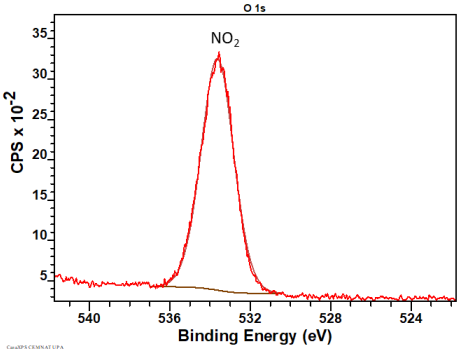
O 1s
NO2
CPS x 10-2
Binding Energy (eV)

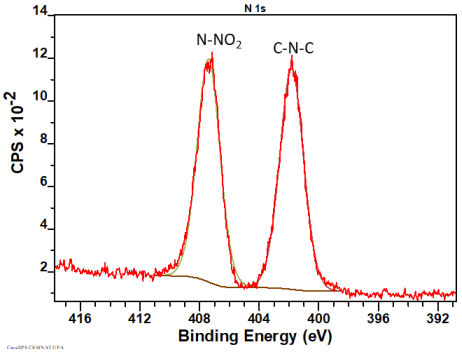
N 1s
N-NO2
C-N-C
CPS x 10-2
Binding Energy (eV)

j) CCs1

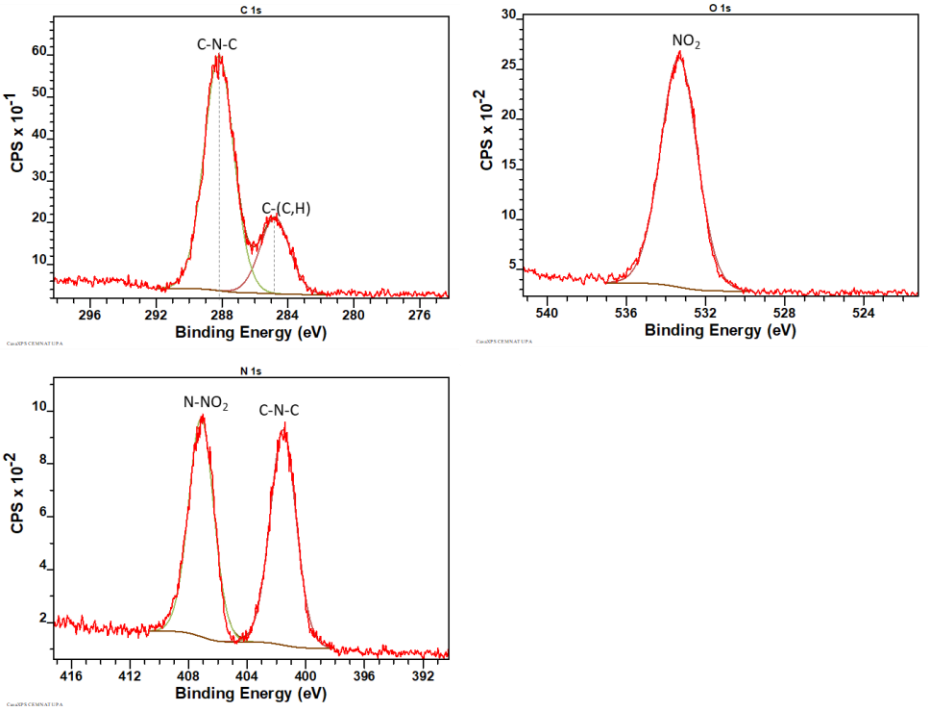

i) TTAZ

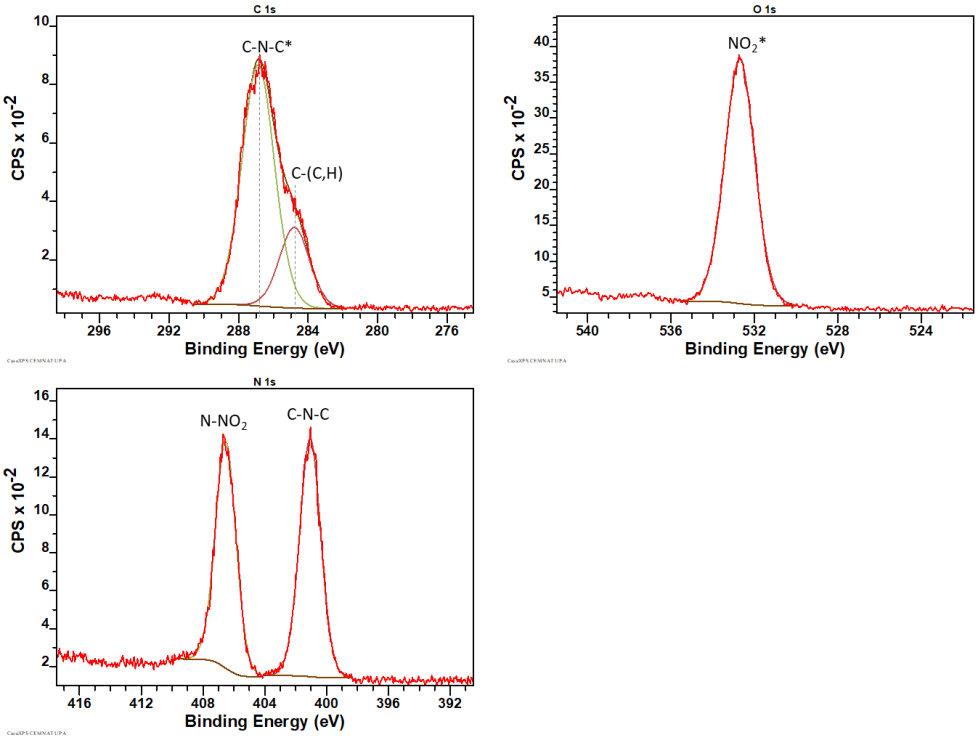

Fig. S4 (a – I) XPS Core levels spectra of pure EMs and their CACs

Table S1 XPS spectra Components Quantification

Sample Identifier	Atomic concentration [%]							Ratios	
	C-(C,H)	C-O	C-N-C	(C=O)-OH	NO_2	C-N-C	N-NO_2	N-NO_2/C-N-C	NO_2/N-NO_2
BCHMX	7.71	-	21.48	-	34.34	17.89	17.04	0.95	2.02
b-CL-20	6.42	1.98	17.42	4.17	34.75	18.06	17.20	0.95	2.02
e-CL-20	6.68	2.14	19.87	1.45	34.33	18.04	17.49	0.97	1.96
S4	6.38	2.00	19.64	2.00	34.01	18.17	17.80	0.98	1.91
S4LV	7.85	1.17	21.04	-	34.72	17.77	17.46	0.98	1.99
S4LZ	9.81	0.71	21.14	-	33.95	17.46	16.93	0.97	2.01
S5	9.62	3.81	16.92	3.42	32.55	17.17	16.50	0.96	1.97
S5LV	5.57	0.61	21.82	-	34.91	18.80	18.30	0.97	1.91
CCs1	7.00	-	21.60	-	35.43	18.10	17.87	0.99	1.98
TTAZ	8.19	-	26.23	-	32.41	17.19	15.98	0.93	2.03

Table S2 XPS spectra Position (Binding energies)

Sample Identifier	Position [eV]						
	C-(C,H)	C-O	C-N-C	(C=O)-OH	NO_2	C-N-C	N-NO_2
BCHMX	284.8	-	288.3	-	533.5	401.8	407.3
b-CL-20	284.8	286.3	288.2	289.6	533.5	401.5	407.2
e-CL-20	284.8	286.3	288.6	290.0	533.8	401.9	407.5
S4	284.8	286.3	288.4	289.7	533.7	401.9	407.3
S4LV	284.8	286.3	288.2	-	533.4	401.6	407.2
S4LZ	284.8	286.3	288.1	-	533.3	401.5	407.1
S5	284.8	286.3	288.3	289.4	533.7	401.9	407.4
S5LV	284.8	286.3	288.4	-	533.6	401.8	407.4
CCs1	284.8	-	288.2	-	533.3	401.5	407.1
TTAZ	284.8	-	286.9*	-	532.7*	401.1*	406.5*

S3.3 Heat of combustion and enthalpy of formation

The heat of combustion, Q_c, was measured with IKA C 200 Bomb-type calorimeter in paper [4]a subsequently from these Q_c values enthalpies of formation where there calculated according to Hess law. To get exact purity of individual and composition of CACs, a chromatographic analysis was carried out in Agilent HPLC 1200 Series with DAD detector. Results are summarized in Table S1.

Hypothetical formulas of CACs, needed for detonation parameters calculation, were calculated [4] from the elemental analysis data of the studied energetic substances. So, that number of nitrogen atoms in the formula of the given mixed BCHMX/CL20crystal is the same as there is in the CL-20) molecule (i.e., of 12). All these results are summariyed in paper [4].

S3.4 Calculation of Detonation Velocities

In framework of paper [4] the theoretical detonation parameters studied samples were calculated (i.e., detonation velocity *D*, detonation pressure *P* and detonation energy E_{det}) by means of the CHEETAH code [13] with the BKWS set of parameters for the BKW (Becker-Kistiakowsky-Wilson) equation of state, that is, $\alpha = 0.5$, $\beta = 0.298$, $\kappa = 1050$, $\Theta = 6{,}620$ [14].

S3.5 Impact sensitivity

The sensitivity was determined employing a standard impact tester with exchangeable anvil (Julius Peters [16, 17]), with the amount of the tested substance being 40 mm^3; the detection was based on sound effect; drop hammers of 2 kg weight were used [15, 16]. The new method/algorithm, called FEST [17] (an innovative method of probit analysis [18]), was utilized to determine the probability levels of the initiation. The obtained sensitivity was expressed as the drop energy, E_{dr}, versus the percentage of initiation. The 50% (E_{dr} 50 %) and 95% (E_{dr} 95 %) probabilities of initiation are specified in this article.

S3.6 Electric spark sensitivity

This sensitivity was determined [19] using a device with electrodes in direct contact with the sample (the ESZ 2000 MIL apparatus of the company OZM Research). The following methodology is taken from paper [19]: a high voltage power supply (operating voltage 4-10 kV) and a set of capacitors of overall capacity in the range from 100 pF to 350 nF produces an electrostatic discharge of total energy from 10 mJ to 16 J. A sample of 1 mm height is fitted into an isolation tube mounted on the lower cylindrical metal electrode. The upper electrode is equipped with manual vertically adjustable positioner. The micro container itself is placed in a separate test box with ventilation. The time behavior of voltage and current at the spark gap is registered with

a scope and than evaluated using a microcomputer to give the effective energy transmitted to the sample.

S3.7 FTIR and Raman spectral studies

A Nicolet Protege 460 FTIR spectrometer was used to record the IR spectral measurements of the samples using the transmission technique. Raman spectra were measured with Nicolet Is50 Raman, Thermo scientific, using an Ar laser (λ = 514.5 nm) and a semiconductor laser (λ= 785 nm). The maximum output power is 1.7 mW of the light spot of the Raman spectrometer, and the spectral resolution is 1 cm^{-1}.

For a detailed understanding of the structural aspects of the CACs prepared and the interactions between their components, the FTIR and Raman spectroscopic techniques were used. For FTIR spectroscopy in Fig. S1 and Table 3, results are summarized for Raman spectroscopy in Fig. S2 and Table 4 (both these data in the main paper text). BCHMX and TTAZ freshly measured remaining taken from earlier reported work [4].

Table S3 A summary of the results of selective stretching vibrations from FTIR and Raman measurements

Assignment	ε-CL-20	β-CL-20	BCHMX	S4 ($CHCl_3$)	S5 (BuOH)	S4LV	S4LZ	S5LV	CCs1	CCs2	TTAZ
FTIR Symmetric N-O stretching	1252	1257	1218	1209	1228	1210	1210	1210	--	1209	1257
FTIR Asymmetric N-O stretching	1562	1253	1562	1553	1554	1554	1554	1553	1556	1553	1283
Raman Ring deformation vibn.	874	867	850	843,	841,	849,	841,	840,	850,	834,	867

S4 Structural characteristics of the starting nitramines and standard DMNA

To better understand the mutual interaction of component molecules in CACs, their spectral data are compared in the main text with characteristics of molecular crystals of these components taken from the CCDC crystal database. The ORTEP views of the used nitramines, serving as references for the main text, are summarized below in their figure forms (Figure S5 – S9)

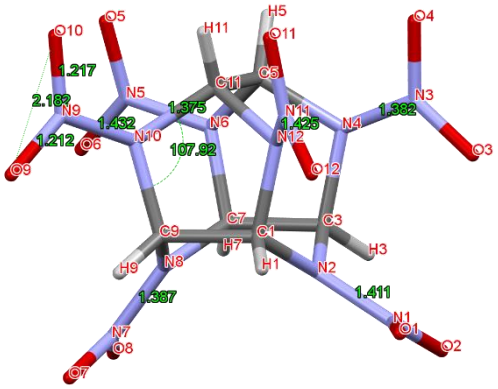

a) ε-CL20 with inter atomic distances [10]

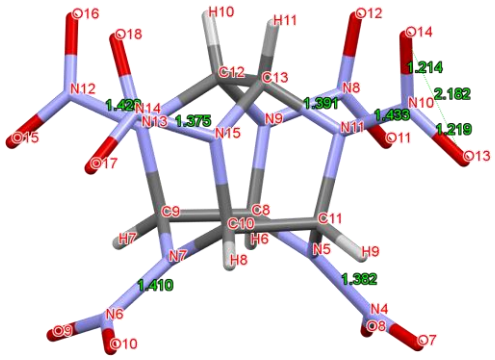

b) β-CL20 with inter atomic distances [19]

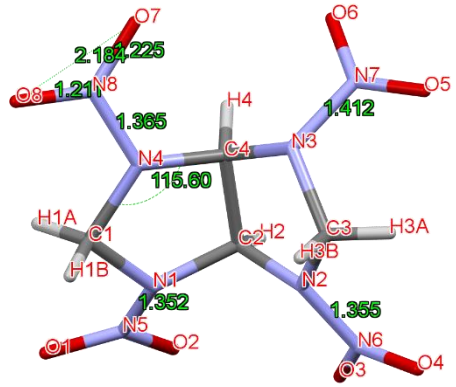

c) BCHMX with inter atomic distances [22]

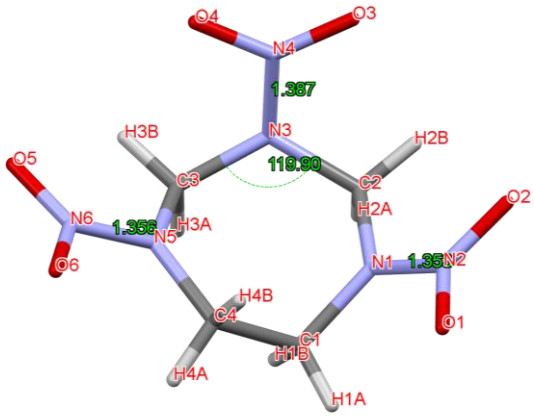

d) TTAZ with inter atomic distances [12]

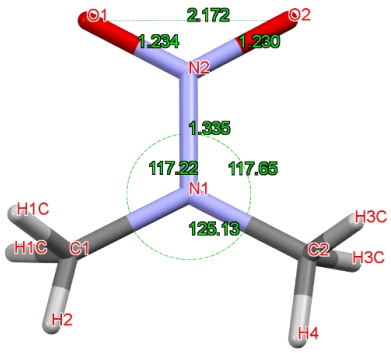

e) DMNA with inter atomic

Fig. S5 (a - e). Nitramines ORTEP 3D molecular structures with their molecular distances in comparison with longest bond with linked bond angle

References

1 Lobanova AA, Sysolyatin SV, Sakovich GV, Zharkov AS, Efimov OA, Popov NI (2012), Process for preparation of 2, 4, 6, 8- tetranitro- 2, 4, 6, 8- tetraazabicyclo[3.3.0] octane by nitration of the corresponding tetrasulfonate salts with nitric acid and nitric anhydride, Russ. Pat. RU 2445311 C1, C07D471/00, JCS Federal Res. & Prod. Center ALTAI, Biysk, (in Russian).

2 Klasovitý D, Zeman S (2010), Process for preparing cis-1,3,4,6-tetranitrooctahydroimidazo-[4,5-d]imidazole (bicyclo-HMX, BCHMX), Czech Pat. 302068, C07D 487/04, (in Czech).

3 Elbei A, Husarová A, Zeman S (2016), Method of preparation of epsilon-2,4,6,8,10,12-hexanitro-2,4,6,8,10,12-hexaazawurtzitane with reduced impact sensitivity, U.S. Patent, US 9,227,981 B2, University of Pardubice.

4 Patil VB, Yan Q-L, Trzcinski WA, Belina P, Shanelova J, Musil T, Zeman S (2022), Co-agglomerated crystals of cyclic nitramines with sterically crowded molecules, CrystEngComm 24:7771–7785, DOI: 10.1039/d2ce00840h.

5 Pati VB, Zalewski K, Schuster J, Belina P, Trzcinski WA, Zeman S (2021), A new insight into the energetic co-agglomerate structures of attractive nitramines, Chem Eng J 420:130472,

6 Xue Z-H, Huang B, Li H, and Yan Q-L (2020), Nitramine-based energetic cocrystals with improved stability and controlled reactivity, Cryst Growth Des 20:8124−8147.

7 Dabir VMB, Viswanath S, Ghosh TK (2018), Hexanitrohexaazaisowurtzitane (HNIW, CL-20); in: Dabir VMB, Viswanath S, Ghosh TK (Eds), Emerging Energetic Materials: Synthesis, Physicochemical, and Detonation Properties, Chapter 2, Springer, pp. 59-100.

8 Woińska M, Grabowsky S, Dominiak PM, Woźniak K, Jayatilaka D (2016), Hydrogen atoms can be located accurately and precisely by X-ray crystallography, Sci Adv 2(5):e1600192.

9 Bolton O, Matzger AJ (2011), Improved stability and smart-material functionality realized in an energetic cocrystal, Angew Chem - Int Ed 50(38):8960–8963.

10 Bolotina NB, Hardie MJ, Speer RL, Pinkerton AA (2004), Energetic materials: Variable-temperature crystal structures of γ- and ε-HNIW polymorphs, J Appl Crystallogr 37(5):808–814.

11 McKinnon JJ, Spackman MA, Mitchell AS (2004), Novel tools for visualizing and exploring intermolecular interactions in molecular crystals, Acta Cryst B Struct Sc*i* 60(6): 627–668, doi: 10.1107/S0108768104020300

12 Zeman S, Atalar T, Růžička A (2020), N-N Bond Lengths and Initiation Reactivity of Nitramines; Cent Eur J Energ Mater 17(2):169-200; DOI 10.22211/cejem/122723

13 Fried LE (1996), CHEETAH 1.39 Users' Manual UCRL-MA-117541, Livermore, CA: Lawrence Livermore National Laboratory.

14 Hobbs ML, Baer MR (1993), Calibrating the BKW-EOS with a large products species base and measured C-J properties, in: Proceedings of the 10th Symposium (International) on Detonation, pp.409-418, Boston.

15 Public Notice of Czech Mining Authority No. 246/1996 Collection of Czech Laws, Establishing more Detailed Conditions for Allowing Explosives, Explosive Objects and Aids into Use, and Their Testing, Aug. 13th, 1996, pp. 3200-3208.

16 Sućeska M (1995), Testing methods of explosives, Heidelberg, Springer; ISBN 0-38794-555-5.

17 Šelešovský J, Pelikan V, Schuster J, Janovský B, Matyáš R (2020), FEST – New procedure for evaluation of sensitivity experiments, Propellants Explos Pyrotech 45:1813–1818.

https://doi.org/10.1002/prep.202000120.

18 Šelešovský J, Pachmáň J (2010), Probit Analysis – a promising tool for evaluation of explosive's sensitivity, Cent Eur J Energet Mater 7(3):269-278.

19 Zeman S, Friedl Z, Kočí J, Pelikán V, Majzlík J (2006),Electric spark sensitivity of nitramines. Part I. Aspects of molecular structure, Cent Eur J Energet Mater *3*(3) 27-44.

20 Klasovitý D, Zeman S, Růžička A, Jungov M, Rohá M (2009), cis-1,3,4,6-Tetranitrooctahydroimidazo-[4,5-d]imidazole (BCHMX), its properties and initiation reactivity, J Hazard Mater 164(2–3):954–961.

21 Krebs B, Mandt J, Cobbledick RE, Small RWH (1979), The structure of N,N-dimethylnitramine; Acta Cryst B35:402-404, https://doi.org/10.1107/S0567740879003630